Inherited retinal degenerations: clinical characterization on the road to therapy

Talib, M.

4.2

The spectrum of structural and functional abnormalities in female carriers of pathogenic variants in the *RPGR* gene

Mays Talib, MD[1], Mary J. van Schooneveld, MD, PhD[2], Caroline Van Cauwenbergh, PhD[3,4], Jan Wijnholds, PhD[1], Jacoline B. ten Brink, BAS[5], Ralph J. Florijn, PhD[5], Nicoline E. Schalij-Delfos, MD, PhD[1], Gislin Dagnelie, PhD[6], RD5000 Consortium, Maria M. van Genderen, MD, PhD[7], Elfride De Baere, MD, PhD[4], Julie de Zaeytijd[3], Frans P.M. Cremers, PhD[8], L. Ingeborgh van den Born, MD, PhD[9], Alberta A. Thiadens, MD, PhD[10], Carel B. Hoyng, MD, PhD[11], Caroline C. Klaver, MD, PhD[10,11,12], Bart P. Leroy, MD, PhD[3,4,13], Arthur A. Bergen, PhD[5,14], Camiel J.F. Boon, MD, PhD[1,2]

Invest Ophthalmol Vis Sci 2018;59(10):4123-4133

1 Department of Ophthalmology, Leiden University Medical Center, Leiden, The Netherlands.
2 Department of Ophthalmology, Academic Medical Center, Amsterdam, The Netherlands.
3 Department of Ophthalmology, Ghent University and Ghent University Hospital, Ghent, Belgium.
4 Center for Medical Genetics, Ghent University and Ghent University Hospital, Ghent, Belgium.
5 Department of Clinical Genetics, Academic Medical Center, Amsterdam, The Netherlands.
6 Wilmer Eye Institute, Johns Hopkins University, Baltimore, Maryland, USA.
7 Bartiméus, Diagnostic Centre for complex visual disorders, Zeist, The Netherlands.
8 Department of Human Genetics and Donders Institute for Brain, Cognition and Behaviour, Radboud University Medical Center, Nijmegen, The Netherlands.
9 Rotterdam Eye Hospital, Rotterdam, The Netherlands.
10 Department of Ophthalmology, Erasmus Medical Center, Rotterdam, The Netherlands.
11 Department of Ophthalmology, Radboud University Medical Center, Nijmegen, The Netherlands.
12 Department of Epidemiology, Erasmus Medical Center, Rotterdam, The Netherlands.
13 Ophthalmic Genetics & Visual Electrophysiology, Division of Ophthalmology, The Children's Hospital of Philadelphia, Philadelphia, Pennsylvania, USA.
14 The Netherlands Institute for Neuroscience (NIN-KNAW), Amsterdam, The Netherlands.

ABSTRACT

Purpose: The purpose of this study was to investigate the phenotype and long-term clinical course of female carriers of *RPGR* mutations.

Methods: This was a retrospective cohort study of 125 heterozygous *RPGR* mutation carriers from 49 families.

Results: Eighty-three heterozygotes were from retinitis pigmentosa (RP) pedigrees, 37 were from cone-/cone-rod dystrophy (COD/CORD) pedigrees, and 5 heterozygotes were from pedigrees with mixed RP/CORD or unknown diagnosis. Mutations were located in exon 1-14 and in ORF15 in 42 of 125 (34%) and 83 of 125 (66%) subjects, respectively. The mean age at the first examination was 34.4 years (range, 2.1 to 86.0). The median follow-up time in heterozygotes with longitudinal data (n = 62) was 12.2 years (range, 1.1 to 52.2). Retinal pigmentary changes were present in 73 (58%) individuals. Visual symptoms were reported in 51 (40%) cases. Subjects with both symptoms and pigmentary fundus changes were older than the other heterozygotes ($p = 0.01$) and had thinner foveal outer retinas ($p = 0.006$). Complete expression of the RP or CORD phenotype was observed in 29 (23%) heterozygotes, although usually in milder forms than in affected male relatives. Best-corrected visual acuity (BCVA) was <20/40 and <20/400 in at least one eye in 45 of 116 (39%) and 11 of 116 (9%) heterozygotes, respectively. Myopia was observed in 74 of 101 (73%) subjects and was associated with lower BCVA ($p = 0.006$). Increasing age was associated with lower BCVA ($p = 0.002$) and decreasing visual field size ($p = 0.012$; I4e isopter).

Conclusions: *RPGR* mutations lead to a phenotypic spectrum in female carriers, with myopia as a significantly aggravating factor. Complete disease expression is observed in some individuals, who may benefit from future (gene) therapeutic options.

INTRODUCTION

Pathogenic variants in the *RPGR* gene are associated with a wide variety of severe X-linked retinal degenerations in male patients, including retinitis pigmentosa (RP3), cone-rod dystrophy (CORD), and isolated cone dystrophy (COD).[1-4] Female carriers of X-linked RP usually experience no or mild symptoms and signs of ocular involvement.[5, 6] However, variable degrees of disease expression have been reported,[2, 7-10] and a few studies have shown a correlation between fundus features and retinal function measures.[10, 11] A pathognomic retinal feature in carriers of X-linked RP is the tapetal-like reflex,[5] a golden metallic-luster sheen of the perimacular retina, but this is often absent or only seen in a subset of female carriers of *RPGR* mutations.[8, 12, 13]

Although a wide spectrum of severity has been described in female carriers from RP pedigrees, female carriers from *RPGR*-associated COD/CORD pedigrees usually display no or mild fundus abnormalities.[14, 15] Genotype-phenotype correlations in female carriers of pathogenic variants in *RPGR*, linking the genotype to the degree of disease expression, have rarely been described, as large cohorts of female heterozygotes are scarce.[10]

The recent initiation of a human gene therapy trial for *RPGR*-associated retinal dystrophies in male patients offers a promising therapeutic perspective (ClinicalTrials.gov number: NCT03116113).[16] An optimal insight into the clinical characteristics and variability of disease expression in female carriers of pathogenic *RPGR* variants becomes increasingly important to further understand the phenotypic spectrum. The purpose of this study was to expand our knowledge of the initial and longitudinal clinical characteristics of a large cohort of female carriers of pathogenic *RPGR* variants, and to assess whether upcoming *RPGR* gene therapy trials may consider the inclusion of affected female carriers.

MATERIALS AND METHODS

Study population

This study identified female carriers of disease-causing *RPGR* variants who underwent at least one clinical examination. Inclusion criteria were a molecular confirmation of an *RPGR* mutation or an obligate carrier status. Additionally, two subjects had not undergone molecular genetic analysis, but an *RPGR* mutation was molecularly confirmed in a first-degree relative, along with the presence of a tapetal-like reflex in the female subject, which is considered a pathognomonic sign of XLRP carriership.[11, 17]

Obligate carriers were defined as daughters of an affected father, mothers of at least two affected sons, or mothers of one affected son along with at least one other affected male patient or confirmed carrier in the family, to exclude the possibility of a *de novo* mutation.

Heterozygotes were collected from the database (Delleman database) for genetic eye diseases at the Academic Medical Center (AMC) in Amsterdam, from various other Dutch medical centers within the framework of the RD5000 consortium,[18] and from the Ghent University Hospital in Belgium. Of the 125 included female carriers of pathogenic *RPGR* variants, 21 were from a large Dutch pedigree that has been previously described,[14] and additional follow-up data since the publication of that study was available in three subjects.

The study was approved by the Medical Ethics Committee of Erasmus Medical Center for the Dutch subjects and by the Ethics Committee of Ghent University Hospital for the Belgian subjects and adhered to the tenets of the Declaration of Helsinki. Dutch participants provided informed consent for the use of their clinical data for research purposes. In Dutch subjects who were no longer traceable, the subject-specific information was deleted after data collection and the subjects were pseudonymized. For Belgian subjects, the local Ethics Committee waivered the need for informed consent on the condition of pseudonymization.

Genetic analysis

Of the 125 heterozygotes, 108 had received molecular confirmation of their carrier status through Sanger direct sequencing (n = 71), linkage analyses (n = 35), or whole exome sequencing (n = 2), 15 were obligate carriers with no further molecular analysis, and two nonobligate carriers had a tapetal-like reflex and were first-degree relatives to patients who had received genetic confirmation of an *RPGR* mutation. Mutational analyses were performed at the AMC in Amsterdam, The Netherlands (n = 77), the Radboud University Medical Center in Nijmegen, The Netherlands (n = 2), Ghent University Hospital, Ghent, Belgium (n = 14), or at the Manchester Centre for Genomic Medicine, Manchester, United Kingdom (n = 15).

Clinical data collection

Medical records were reviewed for symptoms, best-corrected visual acuity (BCVA), biomicroscopy, fundus examination, full-field dark- and light-adapted single flash and 30 Hz electroretinography (ffERG) according to the International Society for Clinical Electrophysiology of Vision standards,[19] Goldmann visual field (GVF) examination, spectral-domain optical coherence tomography (SD-OCT), and fundus autofluorescence (FAF) where available. Color vision testing was performed in 45 subjects, using Hardy-Rand-Rittler plates (n = 24), Ishihara plates (n = 26), Farnsworth Panel D15 testing (n = 33), and Farnsworth Tritan plates (n = 23). GVF areas of the V4e and I4e target were digitized and converted to seeing retinal areas in mm^2, using a method described by Dagnelie.[20] Not all subjects underwent all clinical examinations. All FAF images and most SD-

OCT images (n = 41) were obtained with the Heidelberg Spectralis (Heidelberg Engineering, Heidelberg, Germany). For these patients, retinal thickness measurements and segmentation analyses were obtained using the Spectralis software, measuring the total central retinal thickness (from the inner limiting membrane to the basal membrane), outer nuclear layer thickness, and the outer retinal thickness + RPE complex (from the external limiting membrane to the basal membrane). In the other three subjects SD-OCT images were taken with the Topcon (n = 1; 3D OCT-1000; Topcon Medical Systems, Tokyo, Japan) or Zeiss CIRRUS version 6.0 (n = 2; Carl Zeiss Meditec Inc., Dublin, CA, USA).

We categorized fundus status based on previously used criteria,[10, 11] using clinical notes and fundus photographs: grade 0 (no fundus abnormalities); grade 1 (a tapetal-like reflex without pigmentary changes in the retina); grade 2 (regional pigmentary changes, e.g., bone-spicule-like pigmentation, involving at least two quadrants, and/or macular RPE alterations, with or without a tapetal-like reflex); grade 3 (at least three quadrants of pigmentary changes or RPE atrophy in the periphery).

Statistical analysis

Data were analyzed using SPSS version 23.0 (IBM Corp., Armonk, NY, USA). BCVA was divided into the following categories, based on the World Health Organization criteria, adding a category of "mild visual impairment" (BCVA <20/40 and ≥20/67): normal or subnormal visual acuity (BCVA ≥20/40), low vision (BCVA <20/67 and ≥20/200), severe visual impairment (BCVA <20/200 and ≥20/400), and blindness (BCVA <20/400). For statistical analysis, we converted visual acuities to logMAR. We used the unpaired *t*-test, Mann-Whitney test, and chi-square tests to compare means, medians, and proportions, respectively. Longitudinal changes in BCVA and seeing retinal area were analyzed using linear mixed models.

RESULTS

One hundred twenty-five female carriers from 49 families were investigated. Genetic analysis yielded 39 distinct pathogenic *RPGR* variants (Supplementary Table S1). Mutations were located in exon 1-14 and in ORF15 in 41 of 125 (33%) and 84 of 125 (67%) subjects, respectively. Longitudinal data were available for 62 of 125 subjects (50%). In these subjects, the median follow-up time was 12.2 years (interquartile range [IQR]: 12.8; range, 1.1 to 52.2 years), with a median of 4.5 visits per subject (IQR: 5; range, 2 to 31). The follow-up was significantly longer ($p = 0.001$) and more frequent ($p = 0.001$) in subjects with symptoms or pigmentary fundus changes, and in myopic heterozygotes ($p = 0.01$ and $p = 0.002$). The mean age at the first examination was 34.4 years (SD, 17.8; range, 2.1 to 86.0 years).

Symptoms and fundus features

Of the 49 families, 36 (73%) comprised at least one heterozygote with mild to severe symptoms and/or pigmentary fundus changes. At the most severe end of the spectrum of *RPGR* carrier phenotypes, we identified a subset of heterozygotes (n = 29; from 23 pedigrees; Supplementary Figure S1) who displayed extensive intraretinal pigmentary changes or retinal atrophy in at least two quadrants (n = 29), usually with macular RPE alterations or atrophy (26 of 29; 90%), as well as multiple visual symptoms beyond nyctalopia (n = 29), and objectified visual field restriction (27 of 28; 96%; unavailable in n = 1), and/or a BCVA-based visual impairment in at least one eye (23 of 29; 79%), and significantly attenuated scotopic and/or photopic responses on ERG in all cases where an ERG was available (n = 24). There was a significant difference ($p = 0.01$) in mean age between heterozygotes with both symptoms and pigmentary fundus changes (mean, 45.6 years; SD, 18.1; range, 11.7 to 80.2 years) and the other female carriers (mean, 37.7 years; SD, 15.7; range, 7.0 to 86.0 years).

Symptoms were reported by 51 heterozygotes (41%) and included variable degrees of nyctalopia (n = 40; 32%), subjective visual field restriction (n = 17; 14%), subjective central vision decline (n = 29, 23%), and/or photophobia (n = 20; 16%). The presence of symptoms was not associated with the location of the mutation ($p = 0.20$), and no significant genotype-phenotype correlations were found (Supplementary Table S2).

The presence or absence of a tapetal-like reflex was explicitly reported in 60 cases, and was found to be present in 24 of 60 heterozygotes (40%), with no significant age difference between those with and without a tapetal-like reflex ($p = 0.67$), and no significant association between the presence of the tapetal-like reflex and the development of symptoms ($p = 0.54$) or intra-retinal pigmentary changes ($p = 0.37$).

An adequate assessment of both symptomatology and fundus features could be made in 117 subjects. Heterozygotes were asymptomatic and had no pigmentary fundus changes in 35 of 117 cases (30%). Eighty-two heterozygotes (70%) had some degree of disease expression in the form of symptoms and/or pigmentary changes (Table 1): 9 of 117 heterozygotes (8%) had symptoms associated with a retinal dystrophy, without retinal pigmentary changes; 31 of 117 heterozygotes (26%) had retinal pigmentary changes without symptoms; and 42 of 117 heterozygotes (36%) had both symptoms and retinal pigmentary changes.

Of the heterozygotes with retinal pigmentary changes (n = 73), peripheral and midperipheral pigmentations were more marked in the inferior quadrants of the retina in 14 of 73 (19%).
Applying the fundus grading criteria to the last available fundus examination, we were able to distinguish the fundus grade for 117 of 125 heterozygotes (94%; Table 1). An evident change in fundus grade with time was observed in 8 of 117 heterozygotes (7%), and was based either on the new appearance of retinal pigmentary changes (n = 6) in the third to fifth decade of life or on an

increase of previously observed pigmentary changes (n = 2) from one quadrant or hemisphere to at least three quadrants in the fifth decade of life.
Intra-individual asymmetry in the presence or extent of retinal pigmentary changes was noted in 11 of 117 heterozygotes (9%).

Visual acuity
BCVA in the better seeing eye was generally associated with age (0.8% decline/y; $p = 0.002$) and BCVA was lower in individuals with myopia ($p = 0.006$) and with a mutation in exon 1-14 ($p = 0.0003$), but was not significantly associated with the presence of retinal pigmentary changes ($p = 0.17$). BCVA was impaired in at least one eye in 45 of 116 individuals (39%; Figure 1). Mildly impaired visual acuity and low vision in the better seeing eye were seen from the second decade of life onward, whereas blindness was observed from the sixth decade of life onward. BCVA decline in heterozygotes at the most severe end of the spectrum (i.e., full expression of the RP or CORD phenotype) was 1.9%/y ($p = 0.003$). The median BCVA in Dutch male *RPGR* hemizygotes who were related to these affected female carriers was relatively lower ($p = 0.03$) than in the other male patients, despite no significant age difference ($p = 0.39$). The decimal BCVA in female carriers at the last visit, averaged between eyes, was lower in those with exon 1-14 mutations (median BCVA, 0.55; IQR: 0.6; range, light perception to 1.125) than in those with ORF15 mutations (median BCVA, 0.9; IQR: 0.5; range, light perception to 1.6; $p = 0.002$). However, the median BCVA was also lower in heterozygotes from RP pedigrees ($p = 0.00001$) than in those from COD/CORD pedigrees, and mutations in exon 1-14 were almost exclusively found in RP pedigrees. We therefore investigated these genotype-phenotype correlations further by stratifying between heterozygotes from RP pedigrees and COD/CORD pedigrees and analyzing genotype-phenotype correlations within those groups. After this stratification, no difference between heterozygotes with exon 1-14 and those with ORF15 mutations was found ($p = 0.10$). Color vision testing identified a deuteranopic (n = 3), combination deuteranopic and tritanopic (n = 3), unspecified (n = 5), or total (n = 1) deficiency in 12 of 45 (27%) of subjects.

A strong intraindividual symmetry in BCVA was observed (Spearman's correlation coefficient = 0.65; $p < 0.00001$). An intraindividual difference in BCVA between eyes of ≥15 ETDRS letters (0.3 logMAR) at two consecutive examinations or only examination in the case of one BCVA measurement, was found in 31 of 116 (27%), and was most likely attributable to anisometropic amblyopia (interocular difference of ≥2 diopters [D]; n = 10), amblyopia associated with strabismus (n = 3), amblyopia with unclear cause (n = 4), asymmetry in cataract (n = 1), unilateral stronger disease expression (n = 5), or an unknown cause (n = 8). A myopic refractive error (below -0.75D) was found in 74 of 101 (73%) heterozygotes (Table 1), using the last phakic refractive error in the case of pseudophakia (n = 8) or laser-assisted in situ keratomileusis (n = 4). Myopia-associated posterior staphyloma (n = 4), lacquer cracks (n = 4), Fuchs spot (n = 1), and patchy chorioretinal atrophy (n = 8) were reported in 16 subjects. Anisometropia was present in 34 of 101 (34%) subjects.

Table 1. Clinical characteristics of *RPGR* heterozygotes

Characteristics	All (n = 125)	Origin RP pedigree (n = 83)*	Origin COD/CORD pedigree (n = 37)*	*P*-value
Exon 1-14, n (%)	42 (34)*	38 (46)	-	**<0.00001**
ORF15, n (%)	83 (66)	45 (54)	37 (100)	
Median refractive error (IQR; range), D†	-3.6 (8.6; -21.25D - +4.13D)	-5.5 (8.4; -21.25D +4.13D)	-1.0 (3.4; -17.25D - +2.38D)	**0.01**
High myopia (< -6D), n (%)	36/102* (35)	31/68 (46)	5/29 (17)	**0.007**
Moderate myopia (-3D > SER ≥ -6D), n (%)	22/102 (22)	17/68 (25)	4/29 (14)	
Mild myopia (-0.75D > SER ≥ -3D), n (%)	16/102 (16)	6/68 (9)	8/29 (28)	
≥-0.75D	28/102 (27)	14/68 (21)	12/29 (41)	
Cataract, n (%)	33/107 (31)	27/72 (38)	5/32 (16)	**0.02**
SPC, n	9	8	1	
Other or unspecified, n	24	19	4	
Fundoscopic examination				
Optic disc pallor, n (%)	32/94 (34)	26/58 (45)	6/33 (18)	**0.02**
Peripapillary atrophy, n (%)	36/94 (38)	29/58 (50)	7/33 (21)	**0.02**
Vascular attenuation, n (%)	40/93 (43)	35/62 (56)	5/28 (18)	**0.001**
Fundus grade assessable	117*	79	34	
Grade 0, n (%)	21 (17)	12	8	
Grade 1, n (%)	11 (9)	6	4	
Grade 0 or 1, n (%)‡	12 (10)	8	4	
Grade 2, n (%)	43 (34)	34	8	
Grade 3, n (%)	17 (14)	13	4	
Grade 2 or 3, n (%)‡	13* (10)	6	6	
Pigment changes, any type, n (%)	73/117* (62)	53/79 (67)	17/34 (50)	0.10
Bone spicule-like/round, n (%)	46* (37)	39	6	
Salt-and-pepper, *n* (%)	4 (4)	2	2	
Macular RPE alterations/atrophy, n (%)	40 (32)	31	8	0.08
Mean age at macular RPE involvement ± SD, y (range)	43.6±17.5 (12.2-77.7)	44.1±18.2 (12.2-77.7)	43.2±15.8 (21.4-59.3)	0.90
RPE alterations in periphery, n (%)	37 (29)	23	14	
Tigroid/tessellated fundus, *n* (%)	15 (12)	8	7	

ERG pattern§	59*	44	11	
No abnormalities, n (%)	11 (19)	7 (11)	4 (36)	0.06‖
Subnormal/low-to-normal amplitudes, n (%)	6 (10)*	4	1	
Electronegative, n (%)¶	2 (3)	2	-	
Rod-cone, n (%)	9 (15)	9	-	
Reduced rods and cones, no predominance specified, n (%)	19* (32)	17#	1	
Cone-rod, n (%)	8 (14)	2	4	
Isolated cone reduction, n (%)	2 (3)	1	1	
Nondetectable, n (%)	2 (3)	2	-	

Significant *p* values (<0.05) are indicated in bold. SER, spherical equivalent of the refractive error; SPC, subcapsularis posterior cataract.

* Five heterozygotes with mutations in exon 1-14 (n = 4) or ORF15 (n = 1) were not included in the columns distinguishing based on pedigree (RP or COD/CORD), as the diagnosis in the pedigrees could not be established or confirmed in four subjects, and one heterozygote with a mutation in exon 10 (deletion after exon 10) was from a mixed RP/CORD pedigree.

† Averaged between eyes.

‡ In 18 (20%) carriers, no distinction between fundus grades 0 and 1 (n = 9; 10%) or 2 and 3 (n = 9; 10%) could be made based on the notes in the medical record. In seven (8%) heterozygotes, no sufficient data on their fundus appearance were available to estimate the fundus grade.

§ One of the heterozygotes with nondetectable responses had previously documented rod-cone responses. One heterozygote with anisometropia had significantly reduced rod and cone amplitudes in her highly myopic eye, and normal amplitudes in her mildly myopic eye.

‖ Fisher's exact test.

¶ Markedly reduced b-wave with a response resembling an electronegative ERG.

One heterozygote had significantly reduced rod and cone amplitudes in one eye (OS), but normal amplitudes in OD. Other measures of visual function (GVF, BCVA) in this subject showed marked asymmetry in favor of OD.

Full-field ERG and visual field findings

ERGs, available for 59 heterozygotes, showed significantly reduced amplitudes in various patterns in 42 of 59 (71%) heterozygotes (Table 1), with no significant age difference between heterozygotes with normal and those with attenuated responses (p = 0.9). Pigmentary fundus changes were present in 37 of 42 (88%) heterozygotes with significantly reduced ERG amplitudes, and 32 of 42 (76%) had visual symptoms. Heterozygotes with reduced scotopic or photopic amplitudes were significantly (p = 0.005) more myopic (mean, -8.4 D; SD, 6.1) than those with normal amplitudes (mean, -3.3 D; SD, 3.6), although mild (4 of 13), moderate (2 of 13), and high myopia (3 of 13) were also found in those with normal ERG amplitudes.

Between heterozygotes, little intrafamilial variability was seen, as heterozygotes with abnormal ERGs tended to cluster within families. However, intrafamilial differences between heterozygotes and male hemizygotes were observed: five heterozygotes from different pedigrees had a cone- or cone-rod pattern on ERG whereas their affected male relatives had RP.

Goldmann visual fields, available for 53 heterozygotes (106 eyes), showed variable degrees of sensitivity reduction in 46 of 53 subjects (87%; Supplementary Figure S2; Supplementary Table S3), with a unilateral sensitivity reduction in two subjects and relatively more severely affected superior hemifields in 13 subjects. Age was associated with the I4e isopter size (decline rate 4.9%/y; p = 0.012), but not with the V4e isopter size (p = 0.06).

Of the 90 eyes with variable degrees of sensitivity reduction, 69 (77%) had peripheral retinal pigment changes or chorioretinal atrophy. Heterozygotes had a better preserved visual field than their age-matched affected male relatives, with three exceptions from one family (Supplementary Figure S2).

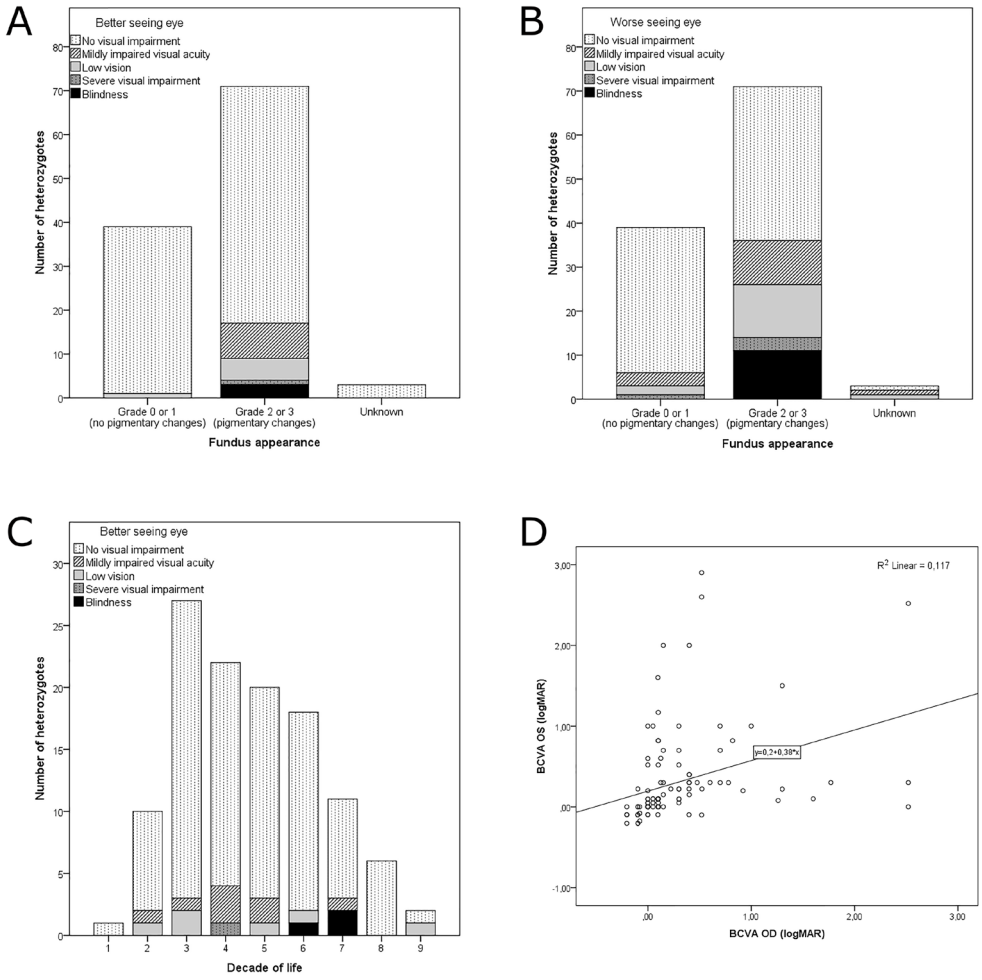

Figure 1. Bar chart of visual impairment category by fundus appearance and by decade of life. Visual impairment in the better (**A**) and worse (**B**) seeing eye, stratified by fundus appearance. **C.** Visual impairment in the better seeing eye, by decade of life, showing a general trend toward visual impairment with increasing age, although the visual acuity in the better seeing eye remains favorable. **D.** The relation of the BCVA in logMAR between the right and left eye, showing a not fully linear relationship. The Spearman's correlation coefficient, taking into account this nonlinear relationship, showed a fair symmetry in visual acuity between eyes (0.64).

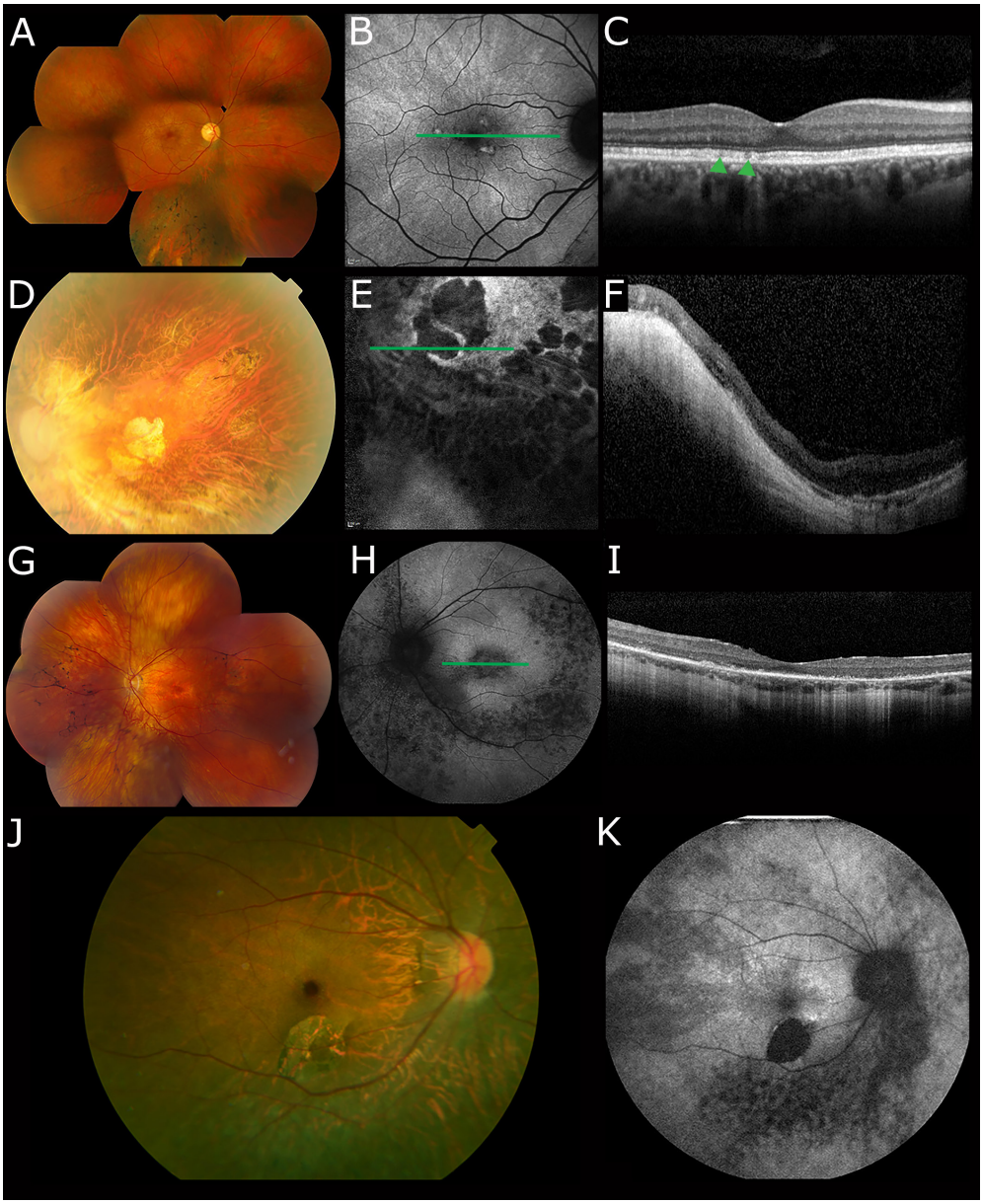

Figure 2. Multimodal imaging illustrating the phenotypical spectrum of *RPGR* heterozygotes from pedigrees of RP. A-C. The right eye of a 48-year-old heterozygote (ORF15: c.2200G>T) with optimal BCVA, sectorial pigmentary changes consistent with RP (**A**). On FAF with a 30° field of view (**B**), a radial pattern of different AF is clearly visible. FAF further shows small hyper-AF spots surrounded by a hypo-AF border, that colocalize with small hyporeflective ellipsoid zone irregularities on SD-OCT (**C**, *green arrowheads*). The appearance of a thick outer plexiform layer may indicate a non-well-aligned scan. **D-F.** The left eye of a 65-year-old highly myopic (-11 D) heterozygote (exon 3: c.248-28_248-10del) with light perception vision OU, showing a posterior staphyloma (**D**), an atrophic retina with

partially obliterated vessels, and bone-spicule pigmentations in the midperiphery (not shown). FAF with a 30° field of view (**E**) shows extensive patches of absent AF, but areas of normo-AF and hyper-AF are visible. SD-OCT (**F**) shows atrophy of all retinal layers, and the ellipsoid zone and external limiting membrane are not discernible. The markedly thinned, almost absent choroid points to an important myopic degenerative factor. **G-I.** The left eye of a 46-year-old moderately myopic heterozygote (ORF15: c.2536G>T) with RP and a decimal BCVA of 0.3/0.5. Her fundus shows vascular attenuation, bone-spicule pigmentation in the midperiphery, and alterations of the RPE in the macula (G). FAF imaging with a 55° field of view (**H**) shows an oval zone of mottled hypo-AF around the fovea, and more coarsely mottled hypo-AF in the perimacula and midperiphery, mainly nasal to the optic disc. The corresponding SD-OCT scan (**I**) shows generalized severe attenuation of the outer retinal layers, with only scattered granular remnants of the ellipsoid zone. The ONL is nearly absent outside of the fovea. **J-K.** The right eye of a 34-year-old highly myopic (-16 D) heterozygote (ORF15: c.2010del), whose fundus photograph (**J**) shows a paracentral patch of retinal atrophy, corresponding on FAF imaging with a 55° field of view (**K**) with a patch of absent AF. FAF further shows a ring of relative hyper-AF surrounding a normal fovea, and mottled areas of hypo-AF around the vascular arcade, more distinctly in the inferior retina.

Findings on retinal imaging

SD-OCT imaging of the macula in 47 heterozygotes showed a preservation of all retinal layers in 22 subjects (15 of 22 with peripheral retinal pigmentary changes; 4 of 22 with central RPE alterations), but showed outer retinal attenuation in 25 heterozygotes (53%), with relative foveal sparing in 23 of these subjects. There was no significant age difference between heterozygotes with outer retinal attenuation on SD-OCT (mean, 44.7 years; SD, 20.3; range, 11.7-80.0 years) and those with normal outer retinas on SD-OCTs (mean, 37.2; SD, 12.8; range, 14.3-59.8 years). Spearman's correlation testing showed no significant correlation between age and central retinal thickness (CRT; $p = 0.81$), foveal outer nuclear layer (ONL) thickness ($p = 0.67$), or thickness of the outer retinal layers ($p = 0.85$). The degree of attenuation varied from mild to moderate peripheral macular thinning of the ellipsoid zone, the external limiting membrane, and/or the outer nuclear layer (n = 12), to a nearly complete absence of these layers with only (para-)foveal remnants (n = 8 complete RP/CORD expression; Figures 2, 3), or a peripheral macular absence of these layers with only foveal and parafoveal granular remnants (n = 2; complete COD/CORD expression; Figure 3), whereas two remaining heterozygotes with RP had no foveal remnants of these layers. One additional subject had unilateral (para-)foveal attenuation of the ellipsoid zone after resolution of a Fuchs spot. No anatomical correlates were observed for the tapetal-like reflex on SD-OCT. Median CRT, ONL, and outer retinal layers + RPE complex thickness measured in the fovea were 220 µm (IQR, 28; range, 126 to 292), 95 µm (IQR, 23; range, 46 to 148), and 96 µm (IQR, 13; range, 42 to 115), respectively. Subjects with symptoms and pigmentary fundus changes had a significantly thinner foveal outer retina ($p = 0.006$), but no significantly thinner CRT ($p = 0.28$) or ONL ($p = 0.21$).

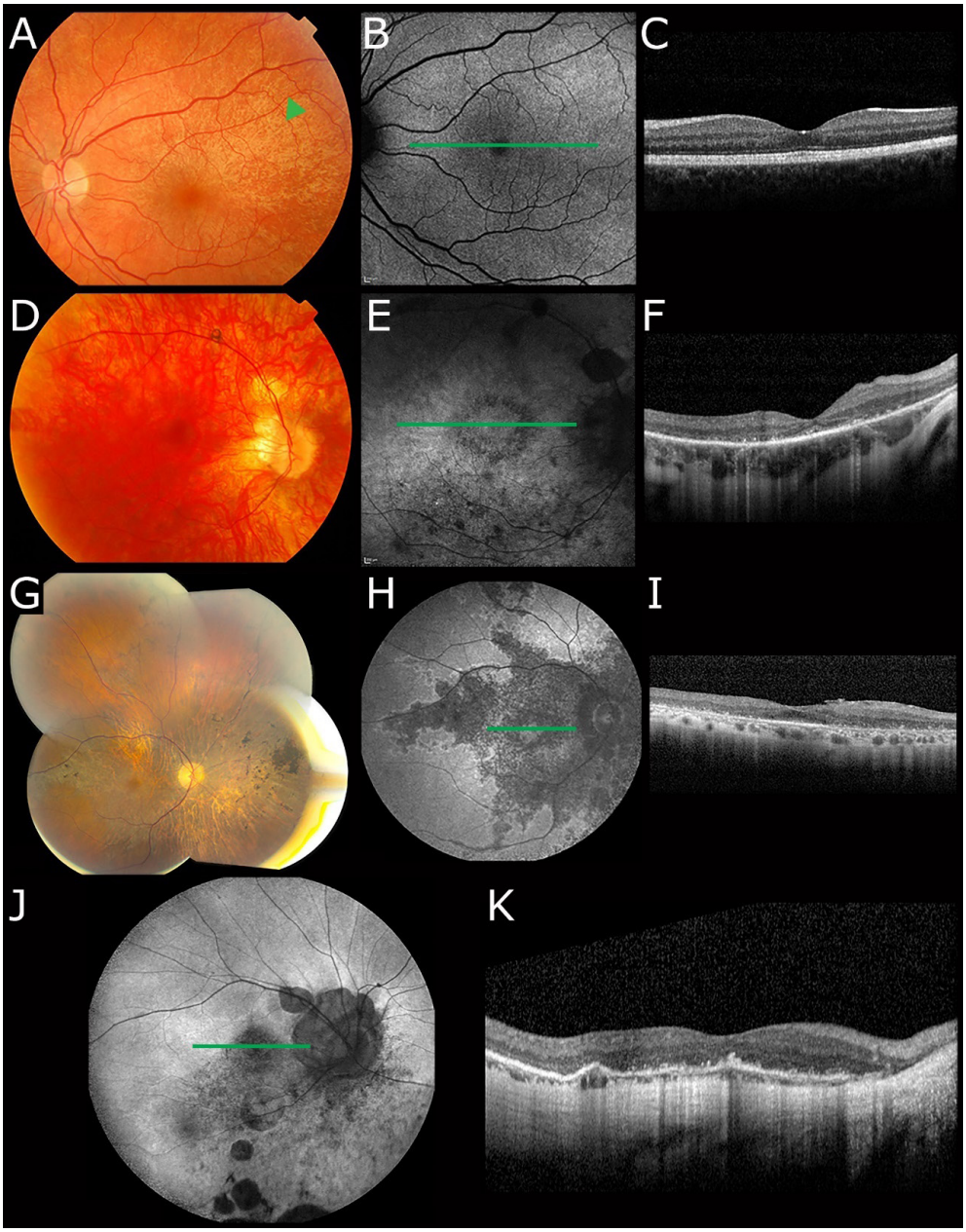

Figure 3. Multimodal imaging illustrating the phenotypical spectrum of *RPGR* heterozygotes from pedigrees of CORD. A-C. The left eye of a 32-year-old heterozygote (ORF15: c.2426_2627del) with optimal BCVA, a tapetal-like reflex on fundus photography (**A**) and FAF with a 30° field of view (**B**), and a normal appearance of the retina on SD-OCT (**C**). **D-F.** The right eye of a highly myopic (-13.5 D) 36-year-old heterozygote (ORF15: c.3092del) with a CORD phenotype and a BCVA of 0.5/0.1, showing peripapillary atrophy and a paravascular patch of chorioretinal atrophy. On FAF with a 30° field of view (**E**), mottled and granular hypo-AF changes are seen, predominantly along the

vascular arcade, with a granular hypo-AF ring around the central macula and a sharply demarcated patch of absent AF along the upper vascular arcade. A radial pattern can be discerned in the perimacular region around the hypo-AF ring. SD-OCT (**F**) shows severe extrafoveal and foveal attenuation of the outer retinal layers, ellipsoid zone, and external limiting membrane, with some granular and mottled remnants of the hyperreflective outer retinal bands. Outside of the fovea, the ONL is barely discernible. **G**-**I.** The right eye of a 63-year-old mildly myopic heterozygote (ORF15: c.2575G>T) with CORD. Fundus photography (**G**) shows extensive outer retinal atrophy in the posterior pole and (mid)periphery, with patches of relatively preserved retina, and bone-spicule pigmentations in the (mid) periphery, encroaching on the posterior pole. FAF with a 55° field of view (**H**) shows a large zone of hypo-AF in the macula, encompassing the peripapillary region and extending into the midperiphery, surrounded by a hyper-AF border. The corresponding SD-OCT scan (**I**) shows an overall attenuation of the outer retina, with granular remnants of the ellipsoid zone. The ONL is discernible in the fovea and direct parafovea but is nearly absent in the perimacula. **J**-**K.** The right eye of a 56-year-old highly myopic (-14.5 D) heterozygote (ORF15: c.3092del; maternal aunt of subject in (**D**-**F**) with CORD, with a BCVA of 0.1 OU. FAF with a 55° field of view of the right eye (**J**) shows peripapillary atrophy, sharply demarcated patches of absent AF along the upper and lower vascular arcade and below the vascular arcade, and a mottled decrease of AF in the posterior pole and below the vascular arcade. Some radial pattern can be detected outside of the vascular pole. SD-OCT (**K**) shows an atrophic ONL, a scarcely visible external limiting membrane, and a granular ellipsoid zone. As in Figure 2F, the thinned choroid points to an important myopic degenerative factor.

FAF imaging in 40 heterozygotes showed abnormalities in 32 subjects (Figures 2, 3), including a radial pattern in 26 of 40, mottled, granular, or patchy hypo-autofluorescent changes including in areas that appeared unaffected on fundoscopy or fundus photography in the posterior pole in 13 of 40, in the periphery in 17 of 40, and patchy areas of absent autofluorescence in seven highly myopic subjects (Figures 2, 3). Of the 26 carriers with a radial pattern on FAF, the tapetal-like reflex had not been detected on fundoscopy or fundus photography in 15 of 26 (58%). In the eight carriers without a radial pattern or other abnormalities on FAF, the fundus showed no RPE changes (n = 4), RPE atrophy in the periphery (n = 1), granular RPE alterations in the central macula (n = 1), or had not been documented (n = 2).

DISCUSSION

In this retrospective cohort study, we describe the phenotypic spectrum of 125 female carriers of pathogenic *RPGR* variants, from 49 pedigrees of RP and COD/CORD. This study is one of the largest studies on female *RPGR* carriers to date, and we identified a number of novel structural and functional characteristics, also in comparison to affected male relatives.

Signs and/or symptoms were common (70%) both in the RP and COD/CORD carrier groups, in carriers of mutations in exon 1-14 as well as in carriers of ORF15 mutations, with complete expression of RP or CORD in 29 heterozygotes (23%). Although the longitudinal results are

probably biased, as the follow-up was significantly longer and more frequent in heterozygotes with myopia or pigmentary changes, our results indicate that clinically severe phenotypes are not rare in heterozygous female *RPGR* mutation carriers.

Female carriers of X-linked retinal dystrophies have been reported to express RP characteristics,[21, 22] sometimes partial or sectorial, albeit in small cohorts.[7, 11, 17, 23] This variability has challenged the ability to identify the accurate disease inheritance mode in families with affected female patients.[24-26] In the early stages of genetic counselling of an RP pedigree, the presence of affected female subjects should raise suspicion of both an autosomal-dominant and an X-linked inheritance mode. In fact, typical RP fundus features, such as bone-spicular or nummular intraretinal pigmentation, optic disc pallor, and vascular attenuation, were common in this cohort, expectedly more so in heterozygotes from RP pedigrees (49%, 44%, and 56%; respectively; Table 1) than in those from COD/CORD pedigrees (18%, 18%, 18%, respectively). Previous reports have shown that female carriers of X-linked COD/CORD usually show either no or minimal fundus changes,[14, 27] but cases of heterozygotes displaying macular RPE alterations have been described,[15] and our cohort further expands this phenotypic spectrum, showing the frequent involvement of macular retina (32%; Table 1), including cases of full COD or CORD expression.

Myopia was associated with a lower BCVA, and high myopia (below -6 D) was found in a similar incidence as in the male cohort we previously investigated (35% in heterozygotes versus 38% in male hemizygotes), with 12% showing a tessellated fundus, four cases of posterior staphyloma, and eight cases of highly myopic patchy chorioretinal atrophy. Although the reasons for the association between *RPGR* mutations and high myopia remain unclear, a recent study analyzing refractive errors in inherited retinal dystrophies has postulated that the transport area between the inner and outer segment (i.e., the location of protein RPGR), is one of the critical sites for refractive error development.[28] Mutations in *RP1* and *RP2*, encoding an outer segment protein and another connecting cilium protein, respectively, have also been linked to high myopia,[29, 30] further corroborating this hypothesis. However, not all genes encoding connecting cilium proteins are associated with myopia, and some have been associated with hyperopia (e.g., *CEP290* and *RPGRIP1*), and biallelic mutations in these are generally associated with much more extreme visual loss due to Leber congenital amaurosis.[31, 32] The presence of (high) myopia in *RPGR* heterozygotes with no photoreceptor dysfunction on ERG supports the notion that photoreceptor degeneration and high myopia might be two parts of the same disease, although the association between high myopia and reduced rod/cone amplitudes would support the concept of scleral remodeling stimulation by signals from dysfunctional photoreceptors and/or more frequent near-focusing due to reduced BCVA. However, the interpretation of the latter is confounded by the association of high and degenerative myopia with reduced ERG amplitudes.[33]

The occurrence of a BCVA below 20/200 in at least one eye (13%; Figure 1) in this cohort was higher than in an earlier longitudinal report in a cohort of XLRP-carriers from a combination of genotyped and ungenotyped families, which reported this BCVA in 2%.[10] In keeping with earlier reports, abnormal GVF (46 of 53; 87%) and ERG (42 of 59; 71%) results were more common than pigmentary changes (73 of 117; 62%) or BCVA impairment (13%, 3%, and 9% low vision, severe visual impairment, or blind in one eye, respectively).[10, 11] However, GVF and ERG were consistently performed only in a subset of heterozygotes, as was the case in this retrospective cohort, and the availability of these test results may thus be subject to bias, as additional testing may have mostly been performed in heterozygotes with symptoms or signs of disease. However, even when assuming that all heterozygotes without additional testing would have no abnormalities, our study shows that a relatively large proportion of heterozygotes experience variable degrees of visual field constriction (46 of 125; 37%) or significant amplitude reduction on ERG (42 of 125; 34%).

Although there was noticeable intrafamilial variability in certain cases, heterozygotes with signs and/or symptoms of disease tended to originate from the same pedigrees. However, this aggregation may be overestimated, as possible (nonobligate) heterozygotes without signs or symptoms may never seek specialist advice from a geneticist or ophthalmologist. The intra- and interfamilial spectrum of severity in heterozygotes of X-linked retinal disorders has been at least partially attributed to the role of X-chromosome inactivation.[34, 35] Based on this X-chromosome inactivation, Dobyns et al.[36] proposed a penetrance and severity index for X-linked diseases, as opposed to using the terminology of X-linked dominant, semidominant, or recessive inheritance, as this concept is not based on X-inactivation in humans, but on the X-transcription speed and dosage compensation in the *Drosophila* model. Random X-inactivation is proposed to occur early in embryonic development, in each cell independently,[37] and would result in a mosaic pattern of cells expressing the normal and mutated gene. Our finding of a radial pattern on the available FAF images in 65% of the examined carriers, even in those who had no tapetal-like reflex on fundoscopy, indicates that FAF may be particularly helpful in detecting such retinal mosaicism. This radial pattern on FAF would support the earlier suggestion that X-inactivation might not occur in each cell independently, but in clusters of cells in a similar pattern,[38] followed by a centrifugal radial growth of the neuroretina during embryonic development.[8] However, random X-inactivation does not fully explain the clustering of nearly complete penetrance in several families in this cohort. There may be a role for skewed X-inactivation, in which the mutant allele is disproportionally (in)active. Extremely skewed X-inactivation has been shown in specific mutations in some non-retinal X-linked disease genes,[39, 40] and has been in favor of the nonmutated allele. Secondary X-inactivation skewing may manifest through a selective (dis)advantage for cells with the mutation-containing X-chromosome,[41] which may be hereditary.[42] The relative family-based, rather than mutation-based, aggregation of affected heterozygotes in this cohort, along with cases of intrafamilial variability, points to a highly likely role of genetic and/or environmental modifiers, as well as potentially skewed X-inactivation. Intraindividual asymmetry was a recurring finding in

this cohort. Left-right asymmetry in X-chromosome inactivation in several paired structures of the body, such as the retina, has been observed, but the biological basis remains unclear. Other than few reports on asymmetrical ERG responses in small numbers of heterozygotes from X-linked RP or COD/CORD pedigrees,[17, 43] this clinical asymmetry has remained largely unexplored. We found a high general correlation between the right and left eye in this cohort, but notable asymmetry in fundus phenotype (9%), in V4e or I4e size on GVF (20%), BCVA (26%), and refractive error (33%) was still observed.

As 23% of heterozygotes display a complete RP or COD/CORD phenotype, with a yearly BCVA decline rate of 1.9%, the question ensues if these heterozygotes may benefit from future therapeutic options. Recently, a submacular gene therapy trial for male patients with *RPGR*-associated RP has commenced,[16] and preclinical studies optimizing subretinal *RPGR* gene therapy have focused on the typical male severe phenotype, which includes an early onset.[44] Inclusion of heterozygotes in gene therapy trials may be challenging until safety and efficacy data are available in male subjects, since male subjects are consistently more severely affected. Nonetheless, in female cases with full disease expression, the macular RPE was frequently altered or atrophic (90% versus 32% of the total cohort), rendering the concept of gene therapy in affected heterozygotes a possibly appropriate treatment option in the future. Serious concerns in the inclusion of female subjects would include the limited comparability to male patients, and the definition of a window of therapeutic opportunity, further complicated by the variability in disease onset and progression. The mean age at which macular RPE involvement was first documented was 43 years, and blind heterozygotes were in their sixth or seventh decade of life, which would translate to a wider window of opportunity in female patients than in the male cohort.

Limitations of this study include its retrospective design, which means that not all subjects had undergone all clinical examinations, as not all clinical examinations were considered relevant or feasible in the clinical setting. While the gathered data are useful, even from subjects with single visits, potential bias should be taken into consideration. Furthermore, as a subgroup of subjects (37 of 125) originated from COD/CORD pedigrees, this compromises the generalizability of the reported findings.

In summary, the findings in this study provide useful insights for the genetic and clinical counselling of female carriers and may have implications for ongoing and future trials. This study displays the wide phenotypic spectrum for *RPGR* heterozygotes and shows that signs and/or symptoms of disease are common, although the visual prognosis is favorable compared with affected males. Myopia is a significant concern due to its effect on BCVA, as it is in affected male patients. A substantial proportion of heterozygotes displays a complete RP or COD/CORD phenotype, and further prospective natural history studies are necessary to determine if inclusion in future (gene) therapeutic trials would be feasible and useful in this subset of severely affected female *RPGR*

mutation carriers, and which outcome measures would provide the most sensitive detection of treatment effect.

Acknowledgements

The authors thank Nicki Hart-Holden, Simon C. Ramsden, and Graeme C. M. Black for the molecular analysis performed at the molecular laboratory of Genetic Medicine, Central Manchester University Hospitals NHS Foundation Trust, Manchester, United Kingdom.

Supported by Stichting Blindenhulp and Janivo Stichting.

REFERENCES

1. Michaelides M, Hardcastle AJ, Hunt DM, Moore AT. Progressive cone and cone-rod dystrophies: phenotypes and underlying molecular genetic basis. Surv Ophthalmol 2006;51:232-58.
2. Pelletier V, Jambou M, Delphin N, et al. Comprehensive survey of mutations in RP2 and RPGR in patients affected with distinct retinal dystrophies: genotype-phenotype correlations and impact on genetic counseling. Hum Mutat 2007;28:81-91.
3. Ayyagari R, Demirci FY, Liu J, et al. X-linked recessive atrophic macular degeneration from RPGR mutation. Genomics 2002;80:166-71.
4. Zito I, Downes SM, Patel RJ, et al. RPGR mutation associated with retinitis pigmentosa, impaired hearing, and sinorespiratory infections. J Med Genet 2003;40:609-15.
5. Fishman GA, Weinberg AB, McMahon TT. X-linked recessive retinitis pigmentosa. Clinical characteristics of carriers. Arch Ophthalmol 1986;104:1329-35.
6. Brouzas D. Psychophysical tests in X-linked retinitis pigmentosa carrier status. Surv Ophthalmol 1995;39 Suppl 1:S76-84.
7. Bird AC. X-linked retinitis pigmentosa. Br J Ophthalmol 1975;59:177-99.
8. Wegscheider E, Preising MN, Lorenz B. Fundus autofluorescence in carriers of X-linked recessive retinitis pigmentosa associated with mutations in RPGR, and correlation with electrophysiological and psychophysical data. Graefes Arch Clin Exp Ophthalmol 2004;242:501-11.
9. Acton JH, Greenberg JP, Greenstein VC, et al. Evaluation of Multimodal Imaging in Carriers of X-Linked Retinitis Pigmentosa. Exp Eye Res 2013;113:41-8.
10. Comander J, Weigel-DiFranco C, Sandberg MA, Berson EL. Visual Function in Carriers of X-Linked Retinitis Pigmentosa. Ophthalmology 2015;122:1899-906.
11. Grover S, Fishman GA, Anderson RJ, Lindeman M. A longitudinal study of visual function in carriers of X-linked recessive retinitis pigmentosa. Ophthalmology 2000;107:386-96.
12. Lorenz B, Andrassi M, Kretschmann U. Phenotype in two families with RP3 associated with RPGR mutations. Ophthalmic Genet 2003;24:89-101.
13. Fishman GA, Grover S, Jacobson SG, et al. X-linked retinitis pigmentosa in two families with a missense mutation in the RPGR gene and putative change of glycine to valine at codon 60. Ophthalmology 1998;105:2286-96.
14. Thiadens AA, Soerjoesing GG, Florijn RJ, et al. Clinical course of cone dystrophy caused by mutations in the RPGR gene. Graefes Arch Clin Exp Ophthalmol 2011;249:1527-35.
15. Ebenezer ND, Michaelides M, Jenkins SA, et al. Identification of novel RPGR ORF15 mutations in X-linked progressive cone-rod dystrophy (XLCORD) families. Invest Ophthalmol Vis Sci 2005;46:1891-8.
16. University of Oxford. New trial for blindness rewrites the genetic code. Available at: http://www.ox.ac.uk/news/2017-03-17-new-trial-blindness-rewrites-genetic-code. Accessed May 17, 2017.
17. Jacobson SG, Yagasaki K, Feuer WJ, Roman AJ. Interocular asymmetry of visual function in heterozygotes of X-linked retinitis pigmentosa. Exp Eye Res 1989;48:679-91.
18. van Huet RA, Oomen CJ, Plomp AS, et al. The RD5000 database: facilitating clinical, genetic, and therapeutic studies on inherited retinal diseases. Invest Ophthalmol Vis Sci 2014;55:7355-60.

19. McCulloch DL, Marmor MF, Brigell MG, et al. ISCEV Standard for full-field clinical electroretinography (2015 update). Doc Ophthalmol 2015;130:1-12.
20. Dagnelie G. Conversion of planimetric visual field data into solid angles and retinal areas. Clin Vis Sci 1990;5:95-100.
21. Al-Maskari A, O'Grady A, Pal B, McKibbin M. Phenotypic progression in X-linked retinitis pigmentosa secondary to a novel mutation in the RPGR gene. Eye (Lond) 2009;23:519-21.
22. Rozet JM, Perrault I, Gigarel N, et al. Dominant X linked retinitis pigmentosa is frequently accounted for by truncating mutations in exon ORF15 of the RPGR gene. J Med Genet 2002;39:284-5.
23. Wu DM, Khanna H, Atmaca-Sonmez P, et al. Long-term follow-up of a family with dominant X-linked retinitis pigmentosa. Eye (Lond) 2010;24:764-74.
24. Almoguera B, Li J, Fernandez-San Jose P, et al. Application of Whole Exome Sequencing in Six Families with an Initial Diagnosis of Autosomal Dominant Retinitis Pigmentosa: Lessons Learned. PLoS One 2015;10:e0133624.
25. Churchill JD, Bowne SJ, Sullivan LS, et al. Mutations in the X-linked retinitis pigmentosa genes RPGR and RP2 found in 8.5% of families with a provisional diagnosis of autosomal dominant retinitis pigmentosa. Invest Ophthalmol Vis Sci 2013;54:1411-6.
26. Sullivan LS, Bowne SJ, Reeves MJ, et al. Prevalence of mutations in eyeGENE probands with a diagnosis of autosomal dominant retinitis pigmentosa. Invest Ophthalmol Vis Sci 2013;54:6255-61.
27. van Everdingen JA, Went LN, Keunen JE, Oosterhuis JA. X linked progressive cone dystrophy with specific attention to carrier detection. J Med Genet 1992;29:291-4.
28. Hendriks M, Verhoeven VJM, Buitendijk GHS, et al. Development of Refractive Errors-What Can We Learn From Inherited Retinal Dystrophies? Am J Ophthalmol 2017;182:81-9.
29. Jayasundera T, Branham KE, Othman M, et al. RP2 phenotype and pathogenetic correlations in X-linked retinitis pigmentosa. Arch Ophthalmol 2010;128:915-23.
30. Chassine T, Bocquet B, Daien V, et al. Autosomal recessive retinitis pigmentosa with RP1 mutations is associated with myopia. Br J Ophthalmol 2015;99:1360-5.
31. Littink KW, Pott J-WR, Collin RWJ, et al. A Novel Nonsense Mutation in CEP290 Induces Exon Skipping and Leads to a Relatively Mild Retinal Phenotype. Invest Ophthalmol Vis Sci 2010;51:3646-52.
32. Walia S, Fishman GA, Jacobson SG, et al. Visual acuity in patients with Leber's congenital amaurosis and early childhood-onset retinitis pigmentosa. Ophthalmology 2010;117:1190-8.
33. Westall CA, Dhaliwal HS, Panton CM, et al. Values of electroretinogram responses according to axial length. Doc Ophthalmol 2001;102:115-30.
34. Koenekoop RK, Loyer M, Hand CK, et al. Novel RPGR mutations with distinct retinitis pigmentosa phenotypes in French-Canadian families. Am J Ophthalmol 2003;136:678-87.
35. Aguirre GD, Yashar BM, John SK, et al. Retinal histopathology of an XLRP carrier with a mutation in the RPGR exon ORF15. Exp Eye Res 2002;75:431-43.
36. Dobyns WB, Filauro A, Tomson BN, et al. Inheritance of most X-linked traits is not dominant or recessive, just X-linked. Am J Med Genet A 2004;129a:136-43.
37. Lyon MF. X-chromosome inactivation and human genetic disease. Acta Paediatr Suppl 2002;91:107-12.

38. Vajaranant TS, Seiple W, Szlyk JP, Fishman GA. Detection using the multifocal electroretinogram of mosaic retinal dysfunction in carriers of X-linked retinitis pigmentosa. Ophthalmology 2002;109:560-8.
39. Plenge RM, Hendrich BD, Schwartz C, et al. A promoter mutation in the XIST gene in two unrelated families with skewed X-chromosome inactivation. Nat Genet 1997;17:353-6.
40. Plenge RM, Tranebjaerg L, Jensen PK, et al. Evidence that mutations in the X-linked DDP gene cause incompletely penetrant and variable skewed X inactivation. Am J Hum Genet 1999;64:759-67.
41. Di Michele DM, Gibb C, Lefkowitz JM, et al. Severe and moderate haemophilia A and B in US females. Haemophilia 2014;20:e136-43.
42. Esquilin JM, Takemoto CM, Green NS. Female factor IX deficiency due to maternally inherited X-inactivation. Clin Genet 2012;82:583-6.
43. Brown J, Jr., Kimura AE, Gorin MB. Clinical and electroretinographic findings of female carriers and affected males in a progressive X-linked cone-rod dystrophy (COD-1) pedigree. Ophthalmology 2000;107:1104-10.
44. Beltran WA, Cideciyan AV, Boye SE, et al. Optimization of Retinal Gene Therapy for X-Linked Retinitis Pigmentosa Due to RPGR Mutations. Mol Ther 2017;25:1866-80.

SUPPLEMENTAL MATERIAL

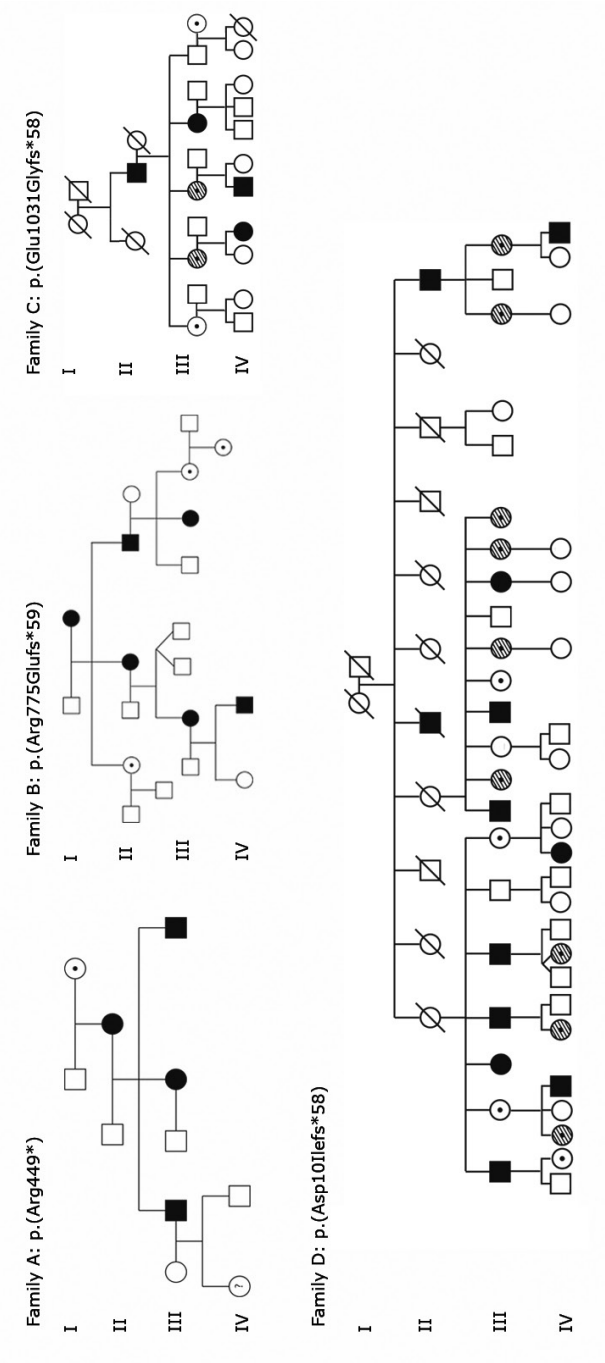

Supplementary Figure S1. Family trees of several female carriers of pathogenic *RPGR* variants. The mutations are depicted in the upper left corner of each family tree. The shaded background on female carriers signifies the presence of symptoms and/or pigmentary fundus changes, and a solid black fill signifies a phenotypical expression at the most severe end of the spectrum, i.e. the presence of visual symptoms beyond nyctalopia, along with intraretinal fundus changes and visual field constriction and/or significantly reduced scotopic and photopic amplitudes.

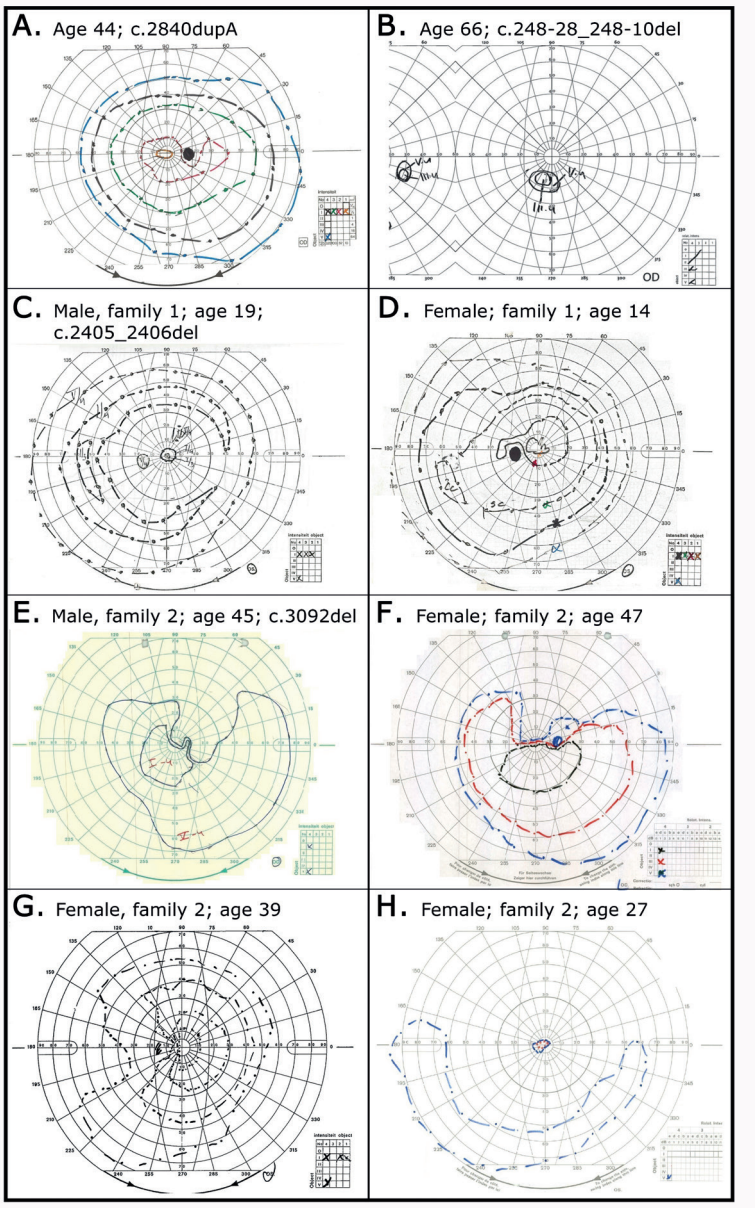

Supplementary Figure S2. Spectrum of visual field decline patterns in female carriers of pathogenic *RPGR* variants. A-B. Goldmann visual fields (GVFs) in individual heterozygotes. **C-D.** GVFs comparing the visual field in a male patient (**C**) with that of his heterozygote sister (**D**). **E-H.** GVFs comparing the visual field in a male patient (**E**) with that of his two carrier daughters (**F**, **G**) and granddaughter (**H**).

Supplementary Table S1. Mutations in the *RPGR* gene found in this cohort

Diagnosis in affected male relatives	Phenotype in female carriers	Exon	Nucleotide	Protein change	N female carriers (n families)
RP	Unaffected 3/15; F 7/15; S 2/15; SF 3/15	1	c.27del	p.(Asp10Ilefs*58)	15 (1)
RP	SF	Intron 1	c.28+2T>C	p.(?)	1
RP	Unaffected		c.112del	p.(Val38Tyrfs*30)	1
RP	SF	3	c.248-28_248-10del	p.(?)	1
Unknown	Unaffected	5	c.329C>A	p.(Ala110Glu)	1
Unknown†	SF	5	c.334_336del	p.(Glu778_799delinsGlu)	1
RP	F 3/3	5	c.425T>G	p.(Ile142Ser)	3 (1)
RP	F	7	c.706C>T	p.(Gln236*)	3 (2)
RP	F 1/3; SF 2/3	8	c.901del	p.(Ser301Leufs*9)	3 (1)
RP	SF 2/2	10‡	c.1060-2A>T	p.(?)	2 (1)
Unknown	NA	10	c.1207C>T	p.(Gln403*)	1
RP	F	10	1246-?_*1091-?	p.(?) deletion after exon 10	1
RP	SF	10	c.1336_1361dup	p.(Asn454Lysfs*31)	1
RP	SF 2/2	11	c.1345C>T	p.(Arg449*)	2 (1)
RP	NA	14	c.1573-?_1753+?del	p.(Lys525Argfs*17)	1
RP	SF	14-ORF15	c.1573-?_3459+?del	p.(?)	1
RP	SF 2/2	14	c.1600C>T	p.(Gln534*)	2 (1)
Unknown	SF	14	c.1685_1686del	p.(His562Argfs*20)	1
RP	Unaffected	ORF15	c.1773_1776del	p.(Gly592Glnfs*9)	1
Unknown	SF	ORF15	c.2010del	p.(Asp671fs)	1
No affected males*	SF	ORF15	c.2200G>T	p.(Glu734*)	1
RP	Unaffected 2/4; SF 1/4; NA ¼	ORF15	c.2237_2241del	p.(Glu746Glyfs*22)	4 (1)
RP	Unaffected ½; SF 1/2	ORF15	c.2257_2260del	p.(Gly753Lysfs*61)	2 (1)
RP		ORF15	c.2323_2324del	p.(Arg775Glufs*59)	5 (1)
RP	Unaffected 2/4; F 2/3	ORF15	c.2362_2366del	p.(Glu788Argfs*45)	4 (2)
RP	Unaffected 6/15; F 4/15; S 1/15; SF in 3/15; NA 1/15	ORF15	c.2405_2406del	p.(Glu802Glyfs*32)	15 (4)
CORD/RP	Unaffected 2/4; F 1/4; SF ¼ (RP)	ORF15	c.2426_2427del	p.(Glu809Glyfs*25)	4 (2)
CORD/RP	Unaffected 1/3; SF 2/3 (RP pedigrees)	ORF15	c.2536G>T	p.(Glu846*)	3 (3)

Supplementary Table S1. Continued

CORD	SF	ORF15	c.2575G>T	p.(Glu859*)	1
RP	Unaffected 2/3; SF 1/3	ORF15	c.2838_2839del	p.(Glu947Glyfs*131)	3 (1)
RP	SF	ORF15	c.2840dup	p.(Glu949Glyfs*130)	4 (1)
CORD	SF	ORF15	c.2872G>T	p.(Glu958*)	1
RP	Unaffected	ORF15	c.2917del	p.(Glu973Lysfs*116)	1
RP	F	ORF15	c.3058del	p.(Glu1020Lysfs*69)	1
CORD	S 1/4; SF 3/4	ORF15	c.3092del	p.(Glu1031Glyfs*58)	4 (1)
COD	S	ORF15	c.3263_3266del	p.(Val1088Alafs*3)	1
COD/CORD	Unaffected 6/21; F 11/21; SF 2/21	ORF15	c.3317dup	p.(Ser1107Valfs*4)	21 (1)
COD/CORD	Unaffected 4/6; SF 2/6 (same pedigree)	ORF15	c.3388_3389del	p.(Leu1130Lysfs*13)	6 (3)

* As reported by subject. S, symptoms only; F, fundus signs only; SF, symptoms and fundus signs; NA, not fully assessable.

† This subject of African descent was adopted and had no knowledge of ophthalmological family history.

‡ Intron 9/exon 10 splice site.

Supplementary Table S2. Clinical characteristics of *RPGR* heterozygotes stratified by genotype

Characteristics	All (n = 125)	Exon 1-14 (n = 42)	ORF15 (n = 83)	*P*-value
Origin RP pedigree, n (%)	83*	38 (46)	45 *(54)	**<0.00001**
Origin COD/CORD pedigree, n (%)	37	-	37 (100)	
Median refractive error (IQR; range), D†	-3.6 (8.6; -21.25D - +4.13D)	-6.1 (8.2; -18.0D - +4.13D)	-2.6 (6.6; -21.25D - +2.9D)	**0.04**
High myopia (< -6D), n (%)	36/101* (36)	17/32 (53)	19/68 (28)	**0.02**
Moderate myopia (-3D > SER ≥ -6D), n (%)	22 (22)	7/32 (22)	14/68 (21)	
Mild myopia (-0.75D > SER ≥ -3D), n (%)	16 (16)	3/32 (9)	13/68 (19)	
≥-0.75D	27 (27)	5/32 (16)	22/68 (32)	
Cataract, n (%)	32/107 (30)	8/34 (24)	24/73 (33)	0.45
SPC, n	9	2	7	
Other or unspecified, n	23	6	17	
Fundoscopic examination				
Optic disc pallor, n (%)	32/94 (34)	13/27 (48)	19/67 (28)	0.10
Peripapillary atrophy, n (%)	36/94 (38)	15/27 (55)	21/67 (31)	0.45
Vascular attenuation, n (%)	40/93 (43)	17/31 (55)	23/62 (37)	0.19
Fundus grade assessable	117	40	77	
Grade 0, n (%)	21 (17)	6	15	
Grade 1, n (%)	11 (9)	2	9	
Grade 0 or 1, n (%)‡	12 (10)	1	11	
Grade 2, n (%)	43 (34)	20	23	
Grade 3, n (%)	17 (14)	8	9	
Grade 2 or 3, n (%)‡	13 (10)	3	10	
Pigment changes, any type, n (%)	73/117 (62)	31/40 (78)	41/77 (53)	**0.02**
Bone spicule-like or round, n	46 (37)	24	22	
Salt-and-pepper, n	4 (4)	1	3	
Macular RPE alterations/atrophy, n	40 (32)	15	25	0.67
RPE alterations in periphery, n	37 (29)	13	24	
Tigroid/tessellated fundus, n	15 (12)	5	10	

Supplementary Table S2. Continued

ERG pattern§	59	23	36	
No abnormalities, *n* (%)	11 (19)	2/23 (9)	9/36 (25)	**0.04‖**
Subnormal/low-to-normal amplitudes, n (%)	6 (10)	2/23	4/36	
Electronegative, n (%)¶	2 (3)	2/23	-	
Rod-cone, n (%)	9 (15)	6/23	3/36	
Reduced rods and cones, no predominance specified, n (%)	19 (32)	10/23#	9/36	
Cone-rod, n (%)	8 (14)	1/23	7/36	
Isolated cone reduction, n (%)	2 (3)	-	2/36	
Nondetectable, n (%)	2 (3)	-	2/36	

Significant *p* values (<0.05) are indicated in bold. SER, spherical equivalent of the refractive error; SPC, subcapsularis posterior cataract.

* Five heterozygotes with mutations in exon 1-14 (n = 4) or ORF15 (n = 1) were not included in the columns distinguishing based on pedigree (RP or COD/CORD), as the diagnosis in the pedigrees could not be established or confirmed in four subjects, and one heterozygote with a mutation in exon 10 (deletion after exon 10) was from a mixed RP/CORD pedigree.

† Averaged between eyes.

‡ In 18 (20%) carriers, no distinction between fundus grades 0 and 1 (n = 9; 10%) or 2 and 3 (n = 9; 10%) could be made based on the notes in the medical record. In seven (8%) heterozygotes, no sufficient data on their fundus appearance were available to estimate the fundus grade.

§ One of the heterozygotes with nondetectable responses had previously documented rod-cone responses. One heterozygote with anisometropia had significantly reduced rod and cone amplitudes in her highly myopic eye, and normal amplitudes in her mildly myopic eye.

‖ Fisher's exact test.

¶ Markedly reduced b-wave with a response resembling an electronegative ERG.

One heterozygote had significantly reduced rod and cone amplitudes in one eye (OS), but normal amplitudes in OD. Other measures of visual function (GVF, BCVA) in this subject showed marked asymmetry in favor of OD.

Supplementary Table S3. Observations on Goldmann visual fields

Observation	N patients (n = 53)
Fully intact visual field for all targets tested	7 (13%)
Intact V4e-I4e; constriction for I3e or I2e and all smaller targets	7 (13%)
Intact V4e; constriction for I4e and all smaller targets	8 (15%)
Constriction for V4e and all smaller targets	31 (58%)
Intraindividual asymmetry*	11 (20%)
Spearman's correlation coefficient V4e isopter size	0.85 ($p < 0.00001$)
Spearman's correlation coefficient I4e isopter size	0.93 ($p < 0.00001$)

*Defined as unilateral constriction, or a difference of >100 mm^2 in the V4e isopter size.